

Antitumor Activity of ZSTK474, a New Phosphatidylinositol 3-Kinase Inhibitor

Shin-ichi Yaguchi, Yasuhisa Fukui, Ichiro Koshimizu, Hisashi Yoshimi, Toshiyuki Matsuno, Hiroaki Gouda, Shuichi Hirono, Kanami Yamazaki, Takao Yamori

Background: We previously synthesized a novel *s*-triazine derivative, ZSTK474 [2-(2-difluoromethylbenzimidazol-1-yl)-4,6-dimorpholino-1,3,5-triazine], that strongly inhibited the growth of tumor cells. We identified its molecular target, investigated its effects on cellular signaling pathways, and examined its antitumor efficacy and toxicity *in vivo*. **Methods:** We used COMPARE analysis of chemosensitivity measurements from 39 human cancer cell lines and identified phosphatidylinositol 3-kinase (PI3K) as a molecular target for ZSTK474. PI3K was immunoprecipitated from A549 cell lysates, and its activity was measured by assessing the incorporation of ³²P into phosphatidylinositol. We used the crystal structure of the PI3K–LY294002 complex to model the binding of ZSTK474 to PI3K (where LY294002 is a known PI3K inhibitor). PI3K downstream activity was analyzed by immunoblotting. Antitumor activity of ZSTK474 was examined against A549, PC-3, and WiDr xenografts in nude mice. Phosphorylation of Akt, a serine/threonine protein kinase and a major signaling component downstream of PI3K, was assessed *in vivo* by immunohistochemistry. **Results:** PI3K was identified as a molecular target for ZSTK474 by COMPARE analysis. We confirmed that ZSTK474 directly inhibited PI3K activity more efficiently than the PI3K inhibitor LY294002. At concentrations of 1 μM, ZSTK474 and LY294002 reduced PI3K activity to 4.7% (95% confidence interval [CI] = 3.2% to 6.1%) and 44.6% (95% CI = 38.9% to 50.3%), respectively, of the untreated control level. Molecular modeling of the PI3K–ZSTK474 complex indicated that ZSTK474 could bind to the ATP-binding pocket of PI3K. ZSTK474 inhibited phosphorylation of signaling components downstream from PI3K, such as Akt and glycogen synthase kinase 3β, and mediated a decrease in cyclin D1 levels. ZSTK474 administered orally to mice had strong antitumor activity against human cancer xenografts without toxic effects in critical organs. Akt phosphorylation was reduced in xenograft tumors after oral administration of ZSTK474. **Conclusion:** ZSTK474 is a new PI3K inhibitor with strong antitumor activity against human cancer xenografts without toxic effects in critical organs. ZSTK474 merits further investigation as an anticancer drug. [J Natl Cancer Inst 2006;98:545–56]

Phosphatidylinositol 3-kinase (PI3K), which is active in signal transduction, generates phosphatidylinositol-3,4,5-trisphosphate (PIP₃) by phosphorylating phosphatidylinositol-4,5-bisphosphate (1,2). PI3K is involved in various cellular processes, including cell survival, vesicle transport, and cytoskeletal rearrangement (3,4). The importance of PI3K in tumorigenesis is supported by the following evidence. The chicken retrovirus ASV16 carries an oncogenic PI3K gene (5), and mutation and/or

amplification of PI3K genes (6–10) has been reported in human and other mammalian cancer cells. Constitutive activation of PI3K may contribute to the malignant phenotype of signet ring carcinomas (11), and PTEN, a PIP₃ phosphatase, has been identified as a tumor suppressor gene (12).

Many clinical studies also indicate that deregulation of PI3K pathway plays a role in various cancers (3,7) and that PI3K may thus be a good target for anticancer drug development (3). Validation of PI3K as a good target for drug development began with the use of dominant-negative mutants and RNA interference studies (13,14). Indeed, a number of compounds have been identified that inhibit PI3K, including wortmannin (15,16), which was originally isolated from soil bacteria and is toxic to fungi; the closely related viridin analogues (17,18); and LY294002, a morpholino derivative of the broad-spectrum kinase inhibitor quercetin (19). Because of inherent difficulties with the stability, solubility, and toxicity of these compounds, efforts are under way to develop new inhibitors of the PI3K pathway (20,21).

In previous work, we synthesized a chemical library of *s*-triazine derivatives and screened these compounds for their ability to inhibit tumor cell growth (22,23). Among more than 1500 *s*-triazine derivatives, we found a new compound, ZSTK474 [2-(2-difluoromethylbenzimidazol-1-yl)-4,6-dimorpholino-1,3,5-triazine], that showed strong antiproliferative activity. However, its molecular target or its potential for a novel anticancer drug was unknown.

We previously established a panel of 39 human cancer cell lines (termed JFCR39) coupled to a drug activity database (24–26) that is comparable to the panel developed by the National

Affiliations of authors: Division of Molecular Pharmacology, Cancer Chemotherapy Center, Japanese Foundation for Cancer Research, Ariake, Koto-ku, Tokyo, Japan (SY, KY, TY); Research Laboratory, Zenyaku Kogyo Co., Ltd., Ohizumi-machi, Nerima-ku, Tokyo, Japan (SY, IK, HY, TM); Laboratory of Biological Chemistry, Department of Applied Biological Chemistry, Faculty of Agricultural and Life Science, Graduate School of Agricultural and Life Science, University of Tokyo, Yayoi, Bunkyo-ku, Tokyo, Japan (YF); The School of Pharmaceutical Sciences, Kitasato University, Shirokane, Minato-ku, Tokyo, Japan (HG, SH).

Correspondence to: Takao Yamori, PhD, Division of Molecular Pharmacology, Cancer Chemotherapy Center, Japanese Foundation for Cancer Research, 3-10-6 Ariake, Koto-ku, Tokyo 135-8550, Japan (e-mail: yamori@jfcrc.or.jp).

See “Notes” following “References.”

DOI: 10.1093/jnci/djj133

© The Author 2006. Published by Oxford University Press. All rights reserved. The online version of this article has been published under an Open Access model. Users are entitled to use, reproduce, disseminate, or display the Open Access version of this article for non-commercial purposes provided that: the original authorship is properly and fully attributed; the Journal and Oxford University Press are attributed as the original place of publication with the correct citation details given; if an article is subsequently reproduced or disseminated not in its entirety but only in part or as a derivative work this must be clearly indicated. For commercial re-use, please contact: journals.permissions@oxfordjournals.org.

Cancer Institute (27,28). We compared cell growth inhibition profiles against the JFCR39 (herein termed fingerprints) of more than 60 standard drugs including doxorubicin, fluorouracil, cytarabine, methotrexate, vincristine, cisplatin, paclitaxel, and irinotecan, by using COMPARE analysis (26), and we showed that COMPARE analysis is an information-intensive approach to identifying the molecular target of a new compound, as described by Paull et al. (28). This system can be used to predict the molecular target or the mode of action of test compounds by assessing the correlation coefficient between the fingerprints mediated by such test compounds and by various reference compounds with known modes of action, including PI3K inhibitors.

The purpose of this study was to identify the molecular target of ZSTK474 with the aid of COMPARE analysis, to investigate the effects of ZSTK474 on cellular signaling pathways, and to examine the antitumor efficacy and toxicity of ZSTK474 in vivo.

MATERIALS AND METHODS

Chemicals

ZSTK116, ZSTK474, ZSTK781, and ZSTK1178 were synthesized in the Research Laboratory, Zenyaku Kogyo Co., Ltd. (Tokyo, Japan). For in vitro studies, these compounds were dissolved in dimethyl sulfoxide. ZSTK474 was suspended in 5% hydroxypropylcellulose in water as a solid dispersion form for animal experiments. Other anticancer drugs and chemicals were purchased as follows: doxorubicin and 5-fluorouracil from Kyowa Hakko Kogyo (Tokyo, Japan); cisplatin from Nippon Kayaku (Tokyo, Japan); irinotecan from Yakult Honsha (Tokyo, Japan); and wortmannin, LY294002, tetramethylrhodamine isothiocyanate-conjugated phalloidin, Igepal CA-630, and platelet-derived growth factor from Sigma (St. Louis, MO).

Cell Lines

A panel of 39 human cancer cell lines (termed JFCR39) (25,26) and B16F10 melanoma cells (29) were previously described. All cell lines were cultured in RPMI 1640 medium supplemented with 5% fetal bovine serum, penicillin (100 U/mL), and streptomycin (100 µg/mL) at 37 °C in humidified air containing 5% CO₂. Cell lines OVCAR3, A549, PC-3, and WiDr, which were used for in vitro detailed analysis or for in vivo study, originated from an ovarian cancer, non-small-cell lung cancer, prostate cancer, and colon cancer, respectively. For in vivo study, A549, PC-3, and WiDr were grown as subcutaneous tumors in nude mice.

Analysis of Cell Proliferation Inhibition

The inhibition of cell proliferation was assessed by measuring changes in total cellular protein in a culture of each cell line in the JFCR panel of cell lines after 48 hours of drug treatment by use of a sulforhodamine B assay (30). The 50% growth inhibition (GI₅₀) value of the drug was calculated as described previously (26,27). The graphic representation of a drug's mean differential growth inhibition for the cell line panel was based on a calculation that used a set of GI₅₀ values, as described previously (28,31). To analyze the correlation between the mean graphs of drug A and drug B, the COMPARE computer algorithm was developed as previously described by Paull et al. (28). The Pearson correla-

tion coefficient between the mean graphs of drug A and drug B was calculated (n = 39).

PI3K Assay in Tumor Cell Extracts

The PI3K assay has been previously described by Fukui et al. (32). In brief, A549 cells were lysed in a buffer containing 20 mM Tris-HCl (pH 7.5), 150 mM NaCl, 5 mM EDTA, and 1% Igepal CA-630 (Sigma), the lysates were centrifuged at 20000g and 4 °C for 10 minutes, and the supernatants were used as cell lysate (protein = 2–4 mg/mL). To immunoprecipitate PI3K, we incubated 200 µL of cell lysate with anti-p85 polyclonal antibody (1:200 dilution; Upstate, Charlottesville, VA) and protein G-agarose (5 µL; Upstate). The anti-p85 polyclonal antibody recognizes the p85 regulatory subunit of PI3K. Class Ia catalytic subunits of PI3K (p110 α , p110 β , and p110 δ) constitutively associate with the p85 subunit. Therefore, PI3K α , PI3K β , and PI3K δ can be immunoprecipitated by the anti-p85 polyclonal antibody. Agarose beads containing immunoprecipitates were washed twice with buffer A (20 mM Tris-HCl at pH 7.5, 150 mM NaCl, 5 mM EDTA, and 1% Igepal CA-630), once with buffer B (500 mM LiCl and 100 mM Tris-HCl at pH 7.5), once with distilled water, and once with buffer C (100 mM NaCl and 20 mM Tris-HCl at pH 7.5). Immunoprecipitates were suspended in 20 µL of buffer C containing phosphatidylinositol at 200 µg/mL. The mixture was preincubated with or without ZSTK474, LY294002, or wortmannin, as indicated, at 25 °C for 5 minutes. [γ -³²P]ATP (2 µCi per assay mixture; final concentration, 20 µM) and MgCl₂ (final concentration, 20 mM) were added to start the reaction. The reaction mixture was incubated at 25 °C for 20 minutes. During this incubation, formation of phosphatidylinositol-3-phosphate was linear (data not shown). Phosphorylated products of phosphatidylinositol were separated by thin-layer chromatography and visualized by autoradiography. The phosphatidylinositol-3-phosphate region was scraped from the plate, and radioactivity was also measured with liquid scintillation spectroscopy (LS6500 Scintillation System; Beckman Instruments, Fullerton, CA). The level of inhibition for each compound was determined as the percentage of ³²P counts per minute obtained without the test compound. To assess the reversibility of PI3K inhibition, the PI3K immunoprecipitates were treated with 1 µM ZSTK474, 10 µM LY294002, or 0.1 µM wortmannin for 5 minutes, and the reaction mixture was divided into two aliquots. One aliquot was washed four times with a buffer containing 100 mM NaCl and 20 mM Tris-HCl (pH 7.5) to remove free ZSTK474, LY294002, or wortmannin from the PI3K, and the PI3K activity of the washed precipitate was measured. The PI3K activity of the other aliquot was measured without washing.

PI3K Assay for Recombinant Catalytic Subunits of PI3K

PI3K assay for recombinant p110, the catalytic subunit of PI3K, was described previously by Gray et al. (33). In a reaction volume of 20 µL, human p110 isoforms β , γ , or δ (Upstate) were incubated with 10 µM phosphatidylinositol-4,5-bisphosphate and 10 µM ATP in assay buffer for 30 minutes at room temperature. Stop buffer (5 µL) containing EDTA and biotinylated PIP₃ was added, followed by 5 µL of detection buffer containing europium-labeled anti-glutathione S-transferase (GST) monoclonal antibody, GST-tagged general receptor for phosphoinositides (GRP1) PH domain, and streptavidin allophycocyanin. Plus

and minus kinase control wells were also included. The plate was read in the time-resolved fluorescence mode, and the homogeneous time-resolved fluorescence (HTRF) signal was determined according to the following formula: $HTRF = 10000 \times (\text{emission at } 665 \text{ nm} / \text{emission at } 620 \text{ nm})$.

Molecular Modeling of the PI3K–ZSTK474 Complex

Conformational analysis of ZSTK474 was performed first with the FlexX docking program (34), which was used to construct a model of the PI3K–ZSTK474 complex structure. This program treats ring systems, such as the morpholino groups in ZSTK474, as rigid structures. The conformational analysis was done with the CAMDAS, version 2.1, program (conformational analyzer with molecular dynamics and sampling) (35). Conditions used for CAMDAS calculation were similar to those described previously (36). Twelve dihedral angles with respect to two morpholino rings were used to cluster similar conformations. As a result of the CAMDAS calculation, 64 different conformers were obtained.

The crystal structure of the PI3K–LY294002 complex (Protein Data Bank Identification Code 1E7V) was used to obtain the PI3K template structure for docking. The docking calculation of each ZSTK474 conformation with PI3K was performed with the FlexX program. A total of 10482 different docking models were generated. Each docking model was then evaluated with the following five different score functions: the F-score (34), the D-score (37), the G-score (38), the ChemScore (39), and the PMF-score (40). These functions were implemented in the SYBYL C-Score module. Finally, a new index, termed the average of auto-scaled score, was calculated to rank all docking models. This index has been recently defined in our laboratory to more adequately rank docking models (41). In the top 20 docking models that were ranked according to the average of auto-scaled scores, all ZSTK474 molecules were found to similarly interact with PI3K. The only difference among the 20 models was with respect to the conformation of the two morpholino rings of ZSTK474. Therefore, we present one of these 20 models, in which two morpholino rings of ZSTK474 take a chair conformation, because this model has the lowest internal energy.

Assay for Chromatin Condensation

OVCAR3 cells were cultured in RPMI 1640 medium supplemented with 5% fetal bovine serum for 24 hours and then cultured for 48 hours with or without 10 μM ZSTK474. Cells were collected, fixed in 1% glutaraldehyde in phosphate-buffered saline (PBS) at 4 °C for 24 hours, stained with 167 μM Hoechst 33342 (Sigma), and examined by fluorescence microscopy to identify apoptotic cells.

Flow Cytometry Analysis

Cells were harvested, washed with ice-cold PBS, and fixed in 70% ethanol. Cells were then washed twice with ice-cold PBS again, treated with RNase A (500 $\mu\text{g}/\text{mL}$; Sigma) at 37 °C for 1 hour, and stained with propidium iodide (25 $\mu\text{g}/\text{mL}$; Sigma). The DNA content of the cells was analyzed with a flow cytometer (FACScalibur, Becton Dickinson, Franklin Lakes, NJ).

Membrane Ruffling

Murine embryonic fibroblasts were treated with or without 1 μM ZSTK474 for 15 minutes and then stimulated with platelet-

derived growth factor (10 ng/mL) for 5 minutes. Cells were fixed with 3% formaldehyde at room temperature for 30 minutes and permeabilized with 0.1% Triton X-100 in PBS for 5 minutes. Filamentous actin in cells was stained with tetramethylrhodamine isothiocyanate-conjugated phalloidin at 0.1 $\mu\text{g}/\text{mL}$, and cells were examined by fluorescence microscopy.

Analysis of PIP₃ Production

PIP₃ production in intact cells was measured as described previously by Kimura et al. (42). In brief, to label murine embryonic fibroblasts, medium was replaced with prewarmed phosphate-free Dulbecco's modified Eagle medium with 25 mM HEPES (pH 7.4) containing [³²P]orthophosphate (0.1 mCi/mL), and cultures were incubated at 37 °C for 4 hours. Lipids were extracted with chloroform and separated by thin-layer chromatography. PIP₃ spots were visualized by autoradiography and identified by standards synthesized by PI3K in vitro (data not shown). Radioactivity in the spots was quantitated with a PhosphorImager SI system (Molecular Dynamics, Sunnyvale, CA).

Western Blot Analysis

A549 cells were lysed in a buffer containing 10 mM Tris–HCl at pH 7.4, 50 mM NaCl, 50 mM NaF, 30 mM sodium pyrophosphate, 50 mM Na₃VO₄, 5 mM EDTA, aprotinin at 100 Kal U/mL, 1 mM phenylmethylsulfonyl fluoride, 0.5% Nonidet P-40, and 0.1% sodium dodecyl sulfate. Proteins in cell lysates were separated by sodium dodecyl sulfate–polyacrylamide gel electrophoresis followed by electroblotting onto a polyvinylidene difluoride membrane (Amersham Biosciences, Piscataway, NJ). Rabbit polyclonal antibodies for Akt, phosphorylated Akt (phosphorylated residue Ser-473), phosphorylated glycogen synthase kinase 3 β (GSK-3 β ; phosphorylated residue Ser-9), phosphorylated FKHR (phosphorylated residue Thr-24)/phosphorylated FKHL1 (phosphorylated residue Thr-32), phosphorylated TSC-2 (phosphorylated residue Ser-1462), phosphorylated mTOR (phosphorylated residue Ser-2448), phosphorylated p70S6K (phosphorylated residue Thr-389), phosphorylated MEK1/2 (phosphorylated residues Ser-217/221), and phosphorylated ERK1/2 (phosphorylated residues Thr-202/Tyr-204) were purchased from Cell Signaling Technology (Beverly, MA) and were diluted 1 : 1000. Rabbit anti-cyclin D1 polyclonal antibody (1 : 200 dilution) was purchased from BioSource International (Camarillo, CA). Horseradish peroxidase–conjugated goat anti-rabbit immunoglobulin G (Cell Signaling Technology) was used as a secondary antibody. Immunoreactive bands were identified with the ECL-plus Western Blotting Detection System (Amersham Biosciences).

Animal Experiments

Animal care and treatment was performed in accordance with the guidelines of the animal use and care committee of the Research Laboratory, Zenyaku Kogyo, and conformed to the NIH *Guide for the Care and Use of Laboratory Animals*. All procedures were approved by the above committee. Male BDF₁ mice and female nude mice with BALB/c genetic backgrounds were purchased from Charles River Japan, Inc. (Yokohama, Japan). Mice were maintained under specific pathogen–free conditions and provided with sterile food and water ad libitum. We used 56 BDF₁ mice. Each BDF₁ mouse was subcutaneously

injected with 5×10^5 B16F10 melanoma cells. Seven days after inoculation, animals were divided randomly into test groups (each with seven mice), and the administration of the drugs, as indicated, began (day 0). ZSTK474 at 100, 200, or 400 mg/kg of body weight was orally administered daily from days 0 to 13. Reference drugs were irinotecan, cisplatin, doxorubicin, and 5-fluorouracil. Each reference drug was administered intravenously from day 0 at the maximum tolerable dose by use of the following optimal schedules: irinotecan at 100 mg/kg administered on days 0, 3, and 7; cisplatin at 10 mg/kg on day 0; doxorubicin at 12 mg/kg on day 0; and 5-fluorouracil at 50 mg/kg on days 0, 3, and 7. Human tumor xenografts were generated with A549 lung cancer cells, PC-3 prostate cancer cells, and WiDr colon cancer cells and were grown as subcutaneous tumors in nude mice. Forty-five nude mice were used in these experiments. Each nude mouse was subcutaneously inoculated with a tumor fragment of $3 \text{ mm} \times 3 \text{ mm} \times 3 \text{ mm}$. When tumors reached a volume of 100–300 mm³, animals were divided randomly into test groups (each with five mice) (day 0). ZSTK474 (400 mg/kg) was administered orally from day 0 until day 13 except for days 3 and 10. For longer administration periods, ZSTK474 at 400 mg/kg was orally administered daily from days 0 to 26, except for days 6, 13, and 20. Then, the mice were photographed on day 28. In another experiment, ZSTK474 at a higher dosage of 800 mg/kg was orally administered in the same schedule, and the body weight changes of the mice were monitored to observe toxicity.

Measurement of Tumor Volume

The length (L) and width (W) of the subcutaneous tumor mass were measured by calipers in live mice, and the tumor volume (TV) was calculated as: $TV = (L \times W^2)/2$. The tumor volume at day n was expressed as relative tumor volume (RTV), according to the formula $RTV = TV_n/TV_0$, where TV_n is the tumor volume at day n , and TV_0 is the tumor volume at day 0. Tumor regression ($T/C\%$) on day 14 was determined by use of the RTV values as follows: $T/C\% = 100 \times (\text{mean } RTV \text{ of treated group})/(\text{mean } RTV \text{ of control group})$. To assess toxicity, we measured the body weight of the tumor-bearing mice. After the chronic administration of ZSTK474, mice were subjected to necropsy examination, including the histopathologic evaluation of bone marrow.

Bone Marrow in Mice Femur

Right-side femurs were fixed with 10% neutral formalin and decalcified with Plank–Rychlo fluid (43). After embedding in paraffin, 3- μm sections of bone marrow were stained with hematoxylin and eosin.

Immunohistochemistry

When the volume of tumors reached 100–300 mm³, ZSTK474 at 400 mg/kg was orally administered once. Mice were killed 4 hours after ZSTK474 administration, and the tumors were excised. Tumor tissue was fixed in 10% neutral formalin and embedded in paraffin. The 6- μm sections were deparaffinized in xylene and then in a 100% to 50% ethanol series. Immunohistochemistry-specific phosphorylated Akt (phosphorylated on Ser-473) antibody and phosphorylated Akt (phosphorylated on Ser-473) blocking peptide were purchased from Cell Signaling Technology. The tissue sections were analyzed by immunohisto-

chemistry for the expression of phosphorylated Akt (Ser-473). For control experiment, phosphorylated Akt (Ser-473) blocking peptide was incubated with phosphorylated Akt (Ser-473) antibody at 4 °C for 2 hours before incubating with the tissue section. The ABC method (Vectastain ABC system kit; Vector Laboratories, Burlingame, CA) was used for immunohistochemical staining, with the sections also being counterstained with hematoxylin.

Statistical Analysis

Pearson correlation coefficients were calculated for the COMPARE analysis and statistical correlation. The two-sided Mann–Whitney U test was used to test the statistical significance of the antitumor efficacy of ZSTK474 in relative tumor growth ratio on days 4, 7, 11, and 14. The number of samples is indicated in the description of each experiment. All statistical tests were two-sided.

RESULTS

Measurement of the Growth-Inhibitory Activity of ZSTK474 and Identification of its Molecular Target

We synthesized and screened a chemical library of *s*-triazine derivatives based on their ability to mediate growth inhibition of tumor cells. We found that ZSTK474 showed potent antiproliferative activity. The chemical structure of ZSTK474 is shown in Fig. 1.

To identify potential molecular targets for ZSTK474, we used COMPARE analysis, an approach that is based on chemosensitivity measurements from the JFCR39 panel of cell lines. We treated cells in the JFCR39 panel with ZSTK474 and examined its effect on cell proliferation. In this way, we obtained the fingerprint for ZSTK474 (Fig. 2). The COMPARE analysis revealed that the fingerprint of ZSTK474 correlated with the fingerprints of no anticancer drug currently in use. However, the fingerprint of ZSTK474 did correlate statistically significantly with that of LY294002, a PI3K inhibitor ($r = .766$ and $P < .001$), as shown in Fig. 2, and with that of wortmannin, another well-characterized PI3K inhibitor ($r = .519$ and $P = .001$). Thus ZSTK474 appears to act as a PI3K inhibitor, although its structure is different from that of LY294002 or of wortmannin (Fig. 1).

We also compared the potency of ZSTK474 in cell growth inhibition with those of LY294002 and wortmannin. The mean logarithm of GI₅₀ for ZSTK474 was -6.49 (at $0.32 \mu\text{M}$ ZSTK474), which was substantially lower than that observed with LY294002 (-5.13 at $7.4 \mu\text{M}$) or wortmannin (-5.00 at $10 \mu\text{M}$), indicating that ZSTK474 had stronger cell growth inhibitory activity than either of these two known PI3K inhibitors.

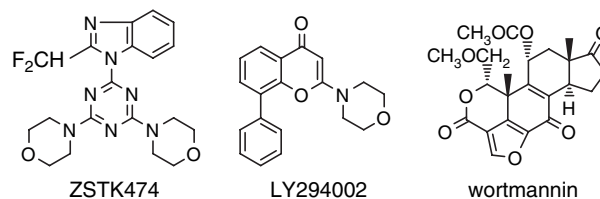


Fig. 1. Chemical structures of the phosphatidylinositol 3-kinase inhibitors ZSTK474, LY294002, and wortmannin. ZSTK474 has one 1-benzimidazolyl and two morpholino groups as substituents on the 1,3,5-triazine ring.

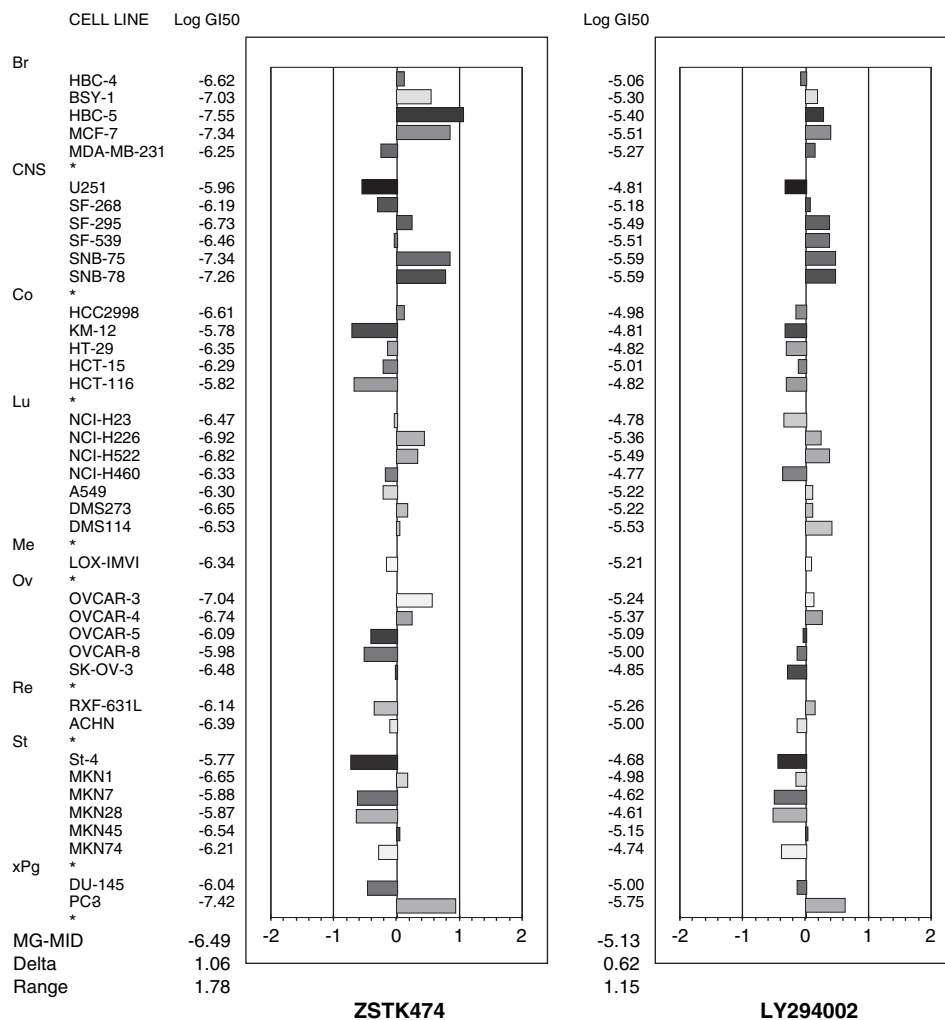


Fig. 2. Growth inhibition activity of ZSTK474 and LY294002 against a panel of 39 human cancer cell lines in the JFCR39 panel. Mean graph was produced by computer processing of the 50% growth inhibition (GI₅₀) values. Logarithm of the GI₅₀ value for each cell line is indicated. In the plot, **columns to the right of zero** indicate that the sensitivity of the cell line to the compound, and **columns to the left** indicate resistance to the compound. The x-axis represents logarithm of difference between the mean of GI₅₀ values for 39 cell lines and the GI₅₀ value for each cell line in the JFCR39 panel. One scale represents one logarithm difference.

MG-MID = mean of logarithm of GI₅₀ values for 39 cell lines in the JFCR39 panel; Delta = logarithm of difference between the MG-MID and the logarithm of the GI₅₀ value for the most sensitive cell line; Range = logarithm of difference between the logarithm of the GI₅₀ value for the most resistant cell line and the logarithm of the GI₅₀ value for the most sensitive cell line. Br = breast; CNS = central nervous system; Co = colon; Lu = lung; Me = melanoma; Ov = ovarian; Re = renal; St = stomach; xPg = prostate. Each **hatch mark** corresponds to the cell line indicated to the left.

Inhibition of PI3K Activity by ZSTK474

We next examined the ability of ZSTK474 to inhibit PI3K activity. We selected A549 cells as the source of PI3K because these cells had an average level of sensitivity to ZSTK474 among cells in the JFCR39 panel. For these experiments, we used PI3K that had been immunoprecipitated from A549 cell lysates with an anti-p85 polyclonal antibody. ZSTK474 inhibited PI3K activity in a dose-dependent manner (Fig. 3, A). At concentrations of 1 μ M, ZSTK474 and LY2194002 reduced the PI3K activity to 4.7% (95% confidence interval [CI] = 3.2% to 6.1%) and 44.6% (95% CI = 38.9% to 50.3%), respectively, of the untreated control activity. The respective concentrations of ZSTK474, LY294002, and wortmannin that inhibited 50% of the PI3K activity (IC₅₀) were 37, 790, and 11 nM. Therefore, as a PI3K inhibitor, ZSTK474 had a 20-fold greater activity than that of LY294002, but its activity was similar to that of wortmannin. However, ZSTK474 reversibly inhibited PI3K activity, as does LY294002, whereas wortmannin irreversibly inhibited PI3K activity (Fig. 3, B).

ZSTK474 did not substantially inhibit the activity of 139 other protein kinases (Supplementary Table 1, available at <http://jncicancerspectrum.oxfordjournals.org/jnci/content/vol98/issue8>), indicating that ZSTK474 is highly specific to PI3K.

There are four subtypes of p110, the catalytic subunit of PI3K— α , β , γ , and δ . The specificity of ZSTK474 to these subtypes was of interest because a high frequency of mutations in the PIK3CA gene, encoding p110 α , in human cancers has been recently reported (7,8). With the PI3K assay described above, it was not possible to determine subtype specificity because the precipitates obtained with the anti-p85 polyclonal antibody could contain a mixture of p110 α , - β , and - δ . To determine the subtype specificity of ZSTK474, we examined ZSTK474 for its activity against recombinant p110 β , - γ , and - δ . We found that ZSTK474 inhibited the activities of p110 β , - γ , and - δ , with respective IC₅₀ values of 17, 53, and 6 nM (Supplementary Fig. 1 available at <http://jncicancerspectrum.oxfordjournals.org/jnci/content/vol98/issue8>), indicating that ZSTK474 was apparently not subtype specific.

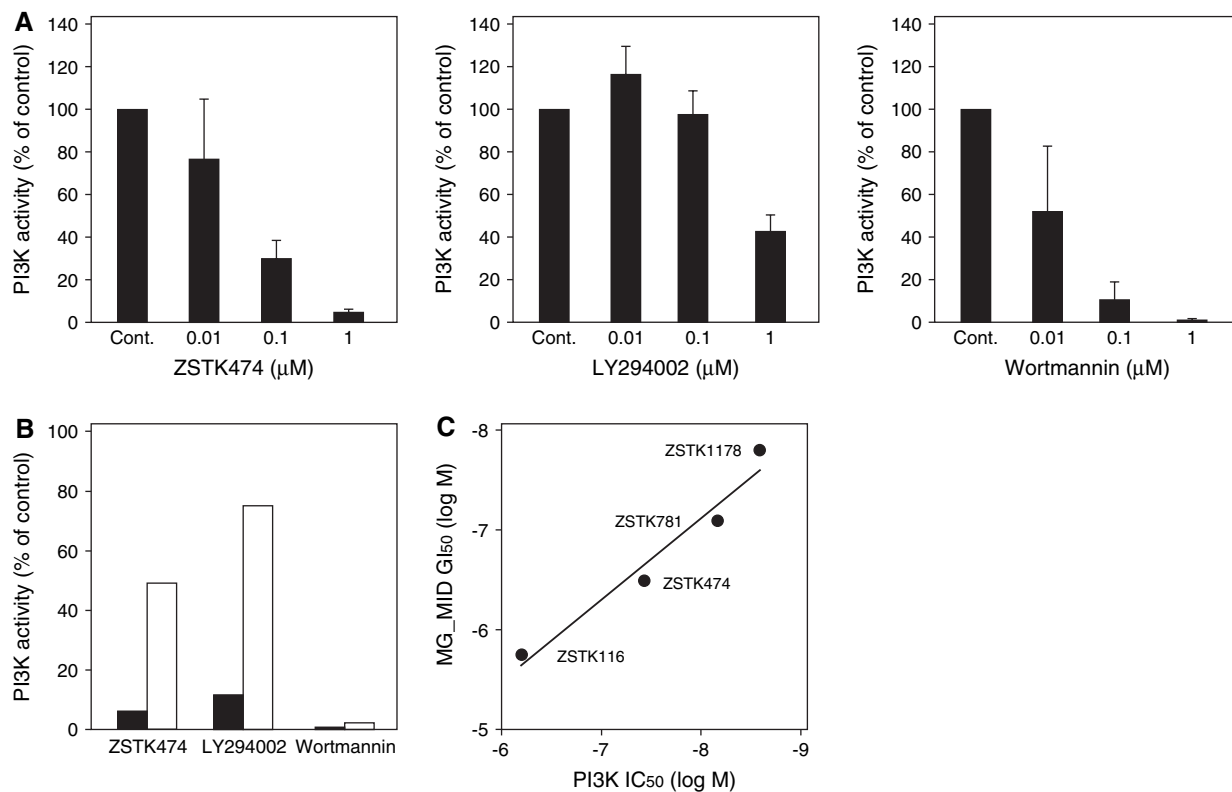


Fig. 3. Effect of ZSTK474 on phosphatidylinositol 3-kinase (PI3K) activity. **A)** Inhibition of PI3K activity. PI3K was immunoprecipitated from A549 cell lysates with anti-p85 polyclonal antibody, and immunoprecipitates were thoroughly washed sequentially with buffer A, buffer B, distilled water, and buffer C. After treatment of the PI3K immunoprecipitates with ZSTK474, LY294002, or wortmannin, as indicated, for 5 minutes, activity was measured by incubating PI3K immunoprecipitates with phosphatidylinositol and [γ -³²P]ATP. Phosphorylated derivatives of phosphatidylinositol were separated by thin-layer chromatography. The radioactivity in all derivatives was measured, and the results are expressed as the percentage of control untreated PI3K activity. Data are the mean of the results of two experiments performed in triplicate. **Error bars** = upper 95% confidence intervals. **B)** Reversibility of PI3K inhibition. The PI3K immunoprecipitates were treated with 1 μ M ZSTK474, 10 μ M LY294002, or 0.1 μ M wortmannin for 5 minutes and

divided into two aliquots. One aliquot was washed four times with a buffer containing 100 mM NaCl and 20 mM Tris-HCl (pH 7.5) to remove free ZSTK474, LY294002, or wortmannin from the PI3K, and PI3K activity of the washed precipitate was measured. The PI3K activity of the other aliquot was measured without washing. The PI3K activity of the immunoprecipitates with (**solid columns**) or without (**open columns**) washing is shown as the percentage of control untreated PI3K activity. Data are the mean of the results of two or three experiments. **C)** Activity of the *s*-triazine derivatives ZSTK116, ZSTK474, ZSTK781, and ZSTK1178. Scattered plot of concentrations of the various derivatives that inhibited 50% of PI3K activity (IC₅₀) versus the mean of logarithm of 50% growth inhibition (GI₅₀) (MG-MID) values of *s*-triazine derivatives. A high and statistically significant correlation ($r = .98$, Pearson correlation coefficient, and $P = .023$) was observed between the two activities ($n = 4$). All statistical tests were two-sided.

Correlation of PI3K Inhibition with Growth-Inhibitory Activity of *s*-Triazine Derivatives

ZSTK474 is an *s*-triazine derivative, as are ZSTK1178, ZSTK781, and ZSTK116, and all have different PI3K inhibitory activities. We investigated whether the PI3K inhibitory activities (IC₅₀) of these four *s*-triazine derivatives were related to their growth inhibitory activities (assessed as the mean logarithm of GI₅₀). A statistically significantly high correlation ($r = .98$ and $P = .023$) was observed between these two inhibitory activities (Fig. 3, C), suggesting that ZSTK474 inhibited cell proliferation by inhibiting PI3K activity.

Molecular Modeling of the PI3K-ZSTK474 Complex

Because all previously described PI3K inhibitors apparently bind to the ATP-binding site of p110, the catalytic subunit of PI3K (44), we investigated whether ZSTK474 also binds to this site by using a model structure, the crystal structure of the PI3K γ -LY294002 complex, to generate a PI3K template structure for docking analysis (44). Analysis of this model structure indicated that there are three hydrogen-bonding interactions between PI3K

and ZSTK474 (i.e., K802 NZ, one of the morpholino oxygens; S806 OG, the other morpholino oxygen; and V882 NH, the benzimidazole nitrogen [Fig. 4, A]).

We next compared the binding modes of ZSTK474 with those of ATP in the active site of PI3K. Two of the three hydrogen bonds between ZSTK474 and PI3K, V882 NH and S806 OG, mimicked those in the ATP-PI3K complex; therefore, the overall arrangements of ZSTK474 and ATP in the PI3K active site are very close (Fig. 4, B). The benzimidazole nitrogen of ZSTK474 forms a hydrogen bond with V882 NH. This hydrogen bond mimics the hydrogen bond between ATP N1 and V882 NH. As discussed previously (45), all kinase inhibitors appear to have a hydrogen bond acceptor in a position equivalent to ATP N1. These features of the ZSTK474-PI3K complex support the hypothesis that ZSTK474 binds to the ATP-binding site of PI3K. In contrast, ZSTK474 and LY294002 appear to bind to different sites in the ATP-binding pocket (Fig. 4, C), with LY294002 forming two hydrogen bonds between PI3K at V882 NH and K833 NZ.

As shown in Fig. 4, D and E, the amino acid residues Met-804 (M804), Trp-812 (W812), and Met-953 (M953) of PI3K create a unique space in the ATP-binding pocket that is larger than the

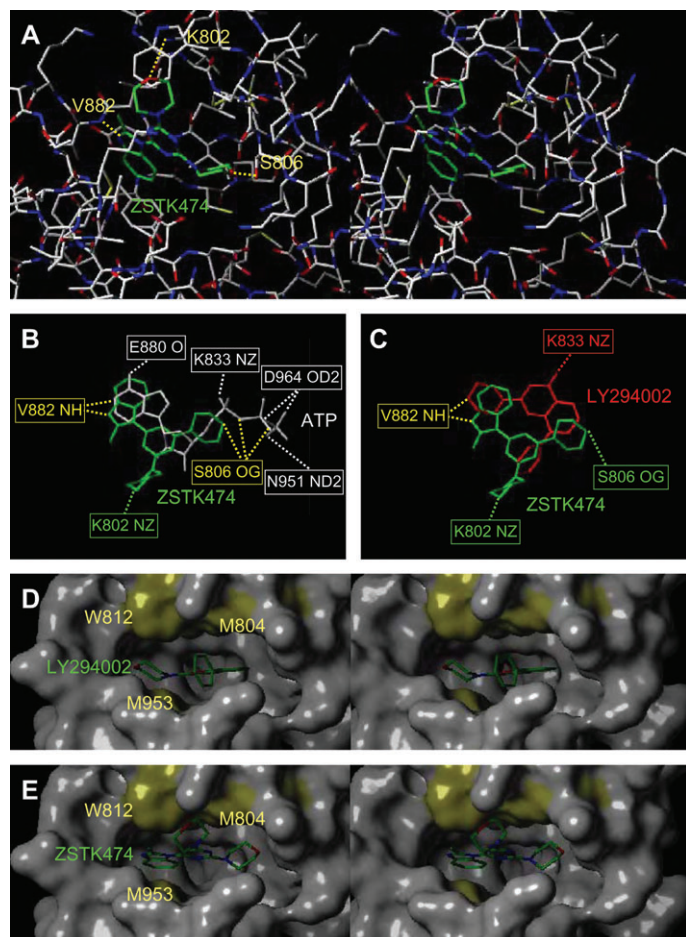


Fig. 4. Molecular modeling of the PI3K–ZSTK474 complex. **A)** Stereo view of the model structure of the PI3K–ZSTK474 complex. Putative hydrogen bonds = **yellow dashed lines**. Carbon atoms of PI3K = **white**; nitrogens = **blue**; oxygens = **red**. **B** and **C)** Binding modes in the PI3K active site. **B)** Comparison of ZSTK474 and ATP. ZSTK474 = **green**; ATP = **white**. **C)** Comparison of ZSTK474 and LY294002. ZSTK474 = **green**; LY294002 = **red**. **D** and **E)** Stereoview of the interactions between PI3K amino acid residues (M804, W812, and M953) and LY294002 or ZSTK474. **D)** LY294002 and PI3K. Amino acid residues = **yellow**; LY294002 = **green**. **E)** ZSTK474 and PI3K. Amino acid residues = **yellow**; ZSTK474 = **green**.

corresponding portion of the ATP-binding pocket of other protein kinases (44). In our models, this space was occupied by the bulky 8-phenyl group of LY294002 (Fig. 4, D), as previously indicated by Walker et al. (44), or by the triazine and morpholino groups of ZSTK474 (Fig. 4, E).

Inhibition of Membrane Ruffling by ZSTK474

It is widely accepted that membrane ruffling is regulated by PI3K by means of a pathway that is independent of Akt, a serine/threonine protein kinase. We examined ZSTK474 for its effect on membrane ruffling induced by platelet-derived growth factor in murine embryonic fibroblast cells. We found that membrane ruffling was induced 5 minutes after platelet-derived growth factor was added to the cultures (Fig. 5, A). When cells were incubated for 15 minutes with 1 μ M ZSTK474 before the addition of platelet-derived growth factor, both membrane ruffling and the formation of PIP₃, a measure of PI3K activity, were blocked (Fig. 5, B). Thus, ZSTK474 appears to inhibit PI3K activity and also to block membrane ruffling.

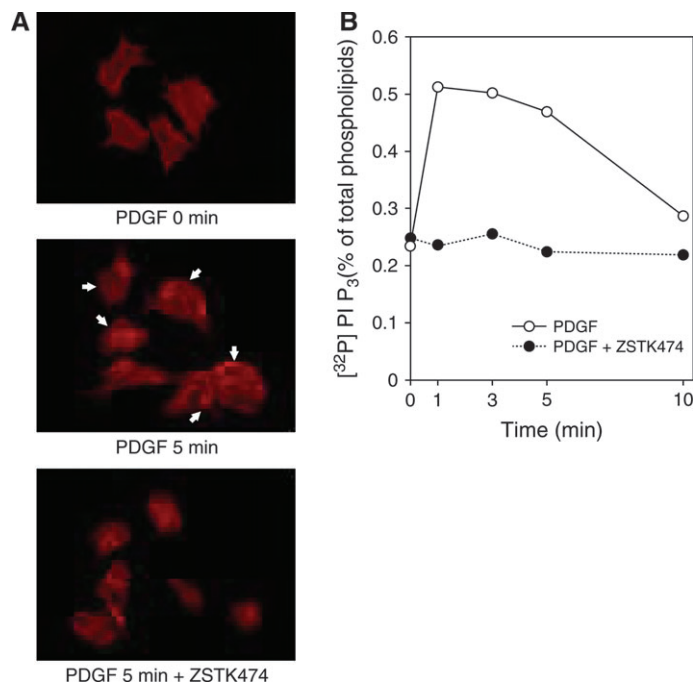


Fig. 5. Effect of ZSTK474 on membrane ruffling and the formation of phosphatidylinositol-3,4,5-trisphosphate (PIP₃). **A)** Inhibition of membrane ruffling in murine embryonic fibroblasts (MEFs) by ZSTK474. MEFs were treated with or without 1 μ M ZSTK474 for 15 minutes and then stimulated with platelet-derived growth factor (10 ng/mL) for 5 minutes. Cells were then fixed and stained for filamentous actin with tetramethylrhodamine isothiocyanate–conjugated phalloidin (**red**). **Arrows** indicate cells with membrane ruffling. **B)** Inhibition of PIP₃ formation by ZSTK474. MEFs were labeled with [³²P]orthophosphate (0.1 mCi/mL) for 4 hours, treated with or without 1 μ M ZSTK474 for 15 minutes, and then stimulated with platelet-derived growth factor (10 ng/mL) as indicated. Radioactivity in the total phospholipids and in PIP₃ was determined with a bioimaging analyzer. Data are the percentage of radioactive PIP₃ as a function of radioactivity in total lipids.

Effects of ZSTK474 on Apoptosis and Cell Cycle

Because PI3K and its downstream components appear to mediate antiapoptotic signals, we examined the effect of ZSTK474 on the induction of apoptosis. At 10 μ M, a higher concentration than its GI₅₀, ZSTK474 induced apoptosis in OVCAR3 cells (Fig. 6, A and B). However, 10 μ M ZSTK474 did not induce apoptosis in A549 cells but instead mediated complete G₁-phase arrest (Fig. 6, C). Therefore, it appears that induction of apoptosis by ZSTK474 is a weak and cell type-dependent event. Here the induction of G₁-phase arrest by ZSTK474 might lead to the inhibition of tumor growth in vivo, which was indeed observed in the animal experiments with A549 below.

Inhibition of Akt Phosphorylation and Downstream Signaling by ZSTK474

The time course of ZSTK474-mediated inhibition of the phosphorylation of Akt, one of the major targets of PI3K, and inhibition of other downstream signaling components was examined in A549 cells by immunoblotting. Treatment with 0.5 μ M ZSTK474 decreased the level of phosphorylated Akt (Ser-473) within 5 minutes without altering overall Akt protein levels and then decreased the level of phosphorylated GSK-3 β (Ser-9) and of cyclin D1 protein expression within 30 minutes (Fig. 7, A). We next investigated the effect of various concentrations of ZSTK474

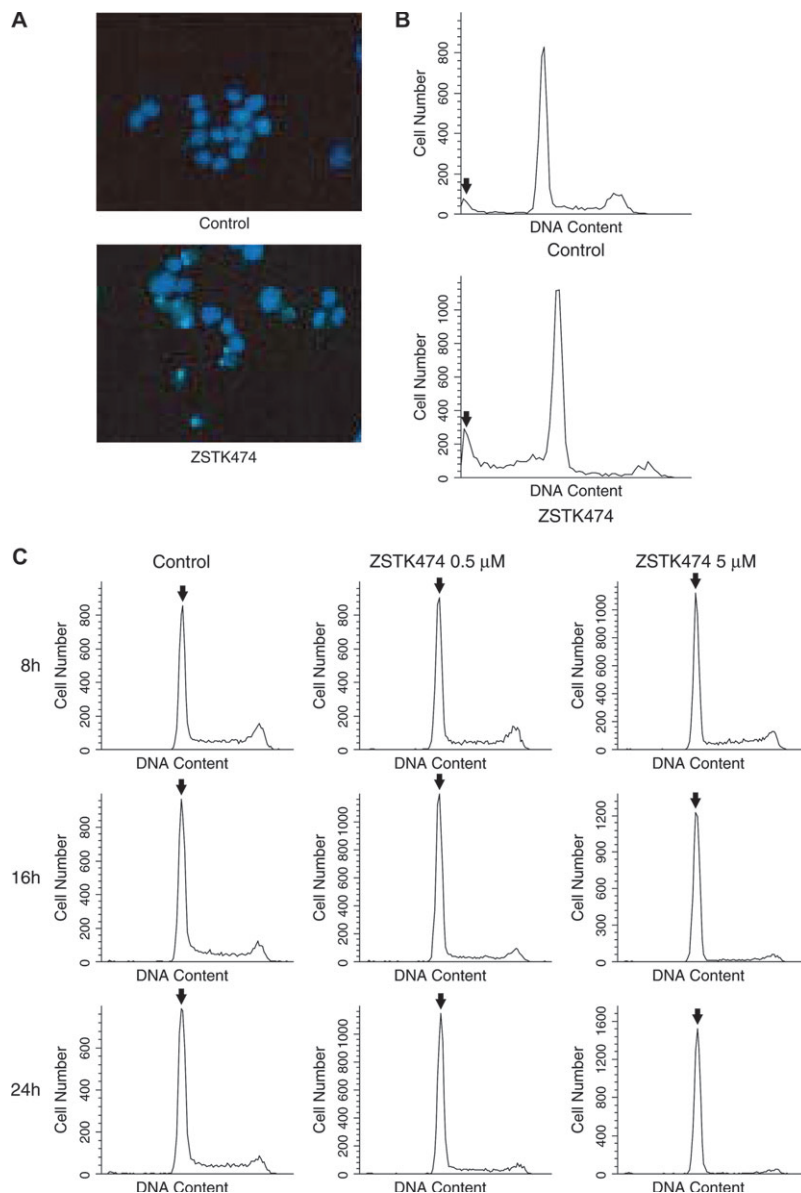


Fig. 6. Effects of ZSTK474 on apoptosis and cell cycle. **A)** Apoptosis assessed by chromatin condensation. OVCAR3 cells were cultured in RPMI 1640 medium supplemented with 5% fetal bovine serum for 24 hours and then cultured for 48 hours with or without 10 μ M ZSTK474. Cells were stained with Hoechst 33342 and examined by fluorescence microscopy. Morphologic changes induced by ZSTK474, such as the condensation of chromatin, were indicative of apoptosis. **B)** Apoptosis as assessed by flow cytometry. OVCAR3 cells cultured under the same conditions as in **panel A** were harvested, washed with ice-cold phosphate-buffered saline (PBS), and fixed in 70% ethanol. Cells were then washed twice with ice-cold PBS again, treated with RNase A (500 μ g/mL, Sigma) at 37 $^{\circ}$ C for 1 hour, and stained with propidium iodide (25 μ g/mL, Sigma). The DNA content of the cells was analyzed with a flow cytometer (FACScalibur, Becton Dickinson). When exposed to ZSTK474, the sub-G₁ peak increased, indicating that ZSTK474 induced apoptosis. **Arrows** indicate the sub-G₁ peaks. **C)** Cell cycle analysis as assessed by flow cytometry. A549 cells were exposed to 0.5 or 5 μ M ZSTK474 for 8, 16, or 24 hours. The DNA content of the cells was determined by flow cytometry as described above. When exposed to ZSTK474, the cell population in G₁ phase increased time dependently, indicating that ZSTK474 blocked the cell cycle at the G₁ phase. **Arrows** indicate the G₁ peaks.

from 0 to 2.0 μ M on the levels of downstream signaling components in the Akt pathway. ZSTK474 inhibited the phosphorylation of forkhead in rhabdomyosarcoma-like 1 (FKHRL1) on Thr-32, forkhead in rhabdomyosarcoma (FKHR) on Thr-24, tuberous sclerosis complex 2 (TSC-2) on Ser-1462, mammalian target of rapamycin (mTOR) on Ser-2448, and p70 ribosomal protein S6 kinase (p70S6K) on Thr-389 and decreased the expression of cyclin D1 protein in a dose-dependent manner (Fig. 7, B). In contrast, phosphorylation of extracellular signal-regulated kinases (ERK1/2) and mitogen-activated protein kinase/extracellular signal-regulated kinase kinases (MEK1/2) were not inhibited by ZSTK474, suggesting that ZSTK474 did not inhibit the RAS-ERK pathway (Fig. 7, A and B). Thus ZSTK474 also appears to act through the Akt pathway.

Antitumor Efficacy of ZSTK474 In Vivo

We evaluated the antitumor activity and toxicity of ZSTK474 by use of a mouse cancer model and three human cancer xenograft models. When administered orally for 2 weeks, ZSTK474

inhibited the growth of subcutaneously implanted mouse B16F10 melanoma tumors in a dose-dependent manner. Almost complete tumor growth inhibition (i.e., tumor regression) was observed at higher dosages. Administration of ZSTK474 at 100, 200, or 400 mg/kg produced tumor regression of 28.5% (95% CI = 21.4% to 35.7%), 7.1% (95% CI = 2.7% to 11.5%), or 4.9% (95% CI = 3.2% to 6.5%) on day 14, respectively. This growth inhibition was superior to that of the four major anticancer drugs examined—irinotecan, cisplatin, doxorubicin, and 5-fluorouracil (each administered at their respective maximum tolerable doses). Tumor regression in mice treated with irinotecan, cisplatin, doxorubicin, or 5-fluorouracil was 96.0% (95% CI = 63.5% to 128.4%), 35.7% (95% CI = 28.6% to 42.9%), 24.0% (95% CI = 16.4% to 31.5%), or 68.3% (95% CI = 21.4% to 115.3%) on day 14, respectively (Fig. 8, A). Moreover, the myelosuppression induced by ZSTK474 at 400 mg/kg was marginal (Fig. 8, B).

We then examined the antitumor activity of ZSTK474 against A549, PC-3, and WiDr human xenografts, which originated from a non-small-cell lung cancer, a prostate cancer, and a colon cancer, respectively. Chronic oral administration of ZSTK474 completely

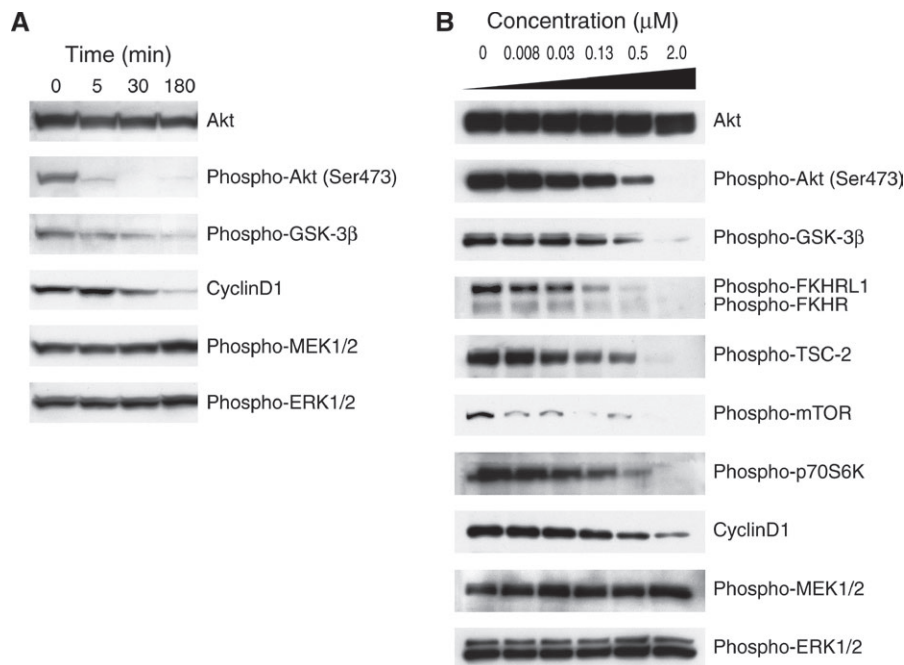


Fig. 7. Immunoblot analysis of Akt and downstream components in the Akt pathway in ZSTK474-treated cells. **A)** Time course. A549 cells were treated with 0.5 μ M ZSTK474 as indicated. **B)** Inhibition as a function of ZSTK474 concentration. A549 cells were treated with the concentration of ZSTK474 indicated for 3 hours. After treatment with ZSTK474, cells were harvested for immunoblot analysis with antibodies specific for nonphosphorylated or phosphorylated proteins indicated of Akt phosphorylation, the level of cyclin D1, and the phosphorylation

of downstream components, including glycogen synthase kinase 3 β (GSK-3 β), extracellular signal-regulated kinases (ERK1/2), mitogen-activated protein kinase/extracellular signal-regulated kinase kinases (MEK1/2), forkhead in rhabdomyosarcoma-like 1 (FKHRL1), forkhead in rhabdomyosarcoma (FKHR), tuberous sclerosis complex 2 (TSC-2), mammalian target of rapamycin (mTOR), and p70 ribosomal protein S6 kinase (p70S6K).

inhibited growth of A549, PC-3, and WiDr xenografts at a dose of 400 mg/kg (Fig. 8, C [upper panels] and D), and it induced the regression of A549 xenograft tumors. To assess toxicity, we measured the body weight of the tumor-bearing mice. Their weight was slightly reduced by administration of ZSTK474, but the reduction was tolerable (no reduction, 17% reduction, and 3% reduction of the day 0 weight on day 14 in A549-bearing mice, in PC-3-bearing mice, in WiDr-bearing mice, respectively) (Fig. 8, C [lower panels]). Dermal toxicity has been reported when LY294002 administered to nude mice (46). However, we observed no dermal toxicity with ZSTK474 even after more than 28 days, as shown in Fig. 8, D. Furthermore, chronic oral administration of ZSTK474 at a higher dose (800 mg/kg) over 4 weeks again reduced body weight within a tolerable range (14% reduction of the day 0 weight on day 28), without toxic effects in critical organs. Thus ZSTK474 appeared to have good therapeutic efficacy in vivo.

Inhibition of the Phosphorylation of Akt by ZSTK474 In Vivo

To confirm that ZSTK474 inhibits the PI3K pathway in vivo, the phosphorylation status of Akt in the subcutaneous A549 tumor tissue was immunohistochemically determined by an anti-Akt antibody specific for phosphorylation at Akt amino acid residue Ser-473. We found that administration of ZSTK474 reduced the level of Akt phosphorylation in tumor tissue (Fig. 8, E).

DISCUSSION

In this study, we demonstrated that a new compound, ZSTK474, is a potent inhibitor of PI3K that differs structurally

from the well-known PI3K inhibitors LY294002 and wortmannin. We also demonstrated that orally administered ZSTK474 has therapeutic efficacy against human cancer xenografts in mice. To the best of our knowledge, this is the first report of an orally administered PI3K inhibitor that has strong antitumor activity without severe toxicity in vivo. The PI3K pathway is activated in various cancer types, and therefore PI3K is a promising therapeutic target of cancer (3,4,21). Thus ZSTK474 appears to be a new anticancer drug candidate targeting PI3K.

From a methodology viewpoint, another novelty of this study is our use of an information-intensive approach, COMPARE analysis, to identify the target of ZSTK474. The COMPARE analysis predicted that the target of ZSTK474 was PI3K, which was later confirmed by direct inhibition of PI3K activity with ZSTK474. We have previously identified the targets of new compounds MS-247 (26) and FJ5002 (47) as topoisomerase I/II and telomerase, respectively, by using COMPARE analysis. This study further confirms that the COMPARE analysis is a powerful tool that can predict the molecular targets of new compounds.

Molecular modeling of the PI3K-ZSTK474 complex indicated that ZSTK474 could bind to the ATP-binding pocket of PI3K through three hydrogen bonds, which is a finding consistent with the ZSTK474-mediated inhibition of PI3K being reversible. Because ZSTK474 formed three hydrogen bonds with PI3K, instead of the two hydrogen bonds formed between LY294002 and PI3K, ZSTK474 appears to be a stronger competitor for the ATP-binding pocket of PI3K than LY294002. Indeed, the PI3K inhibitory activity of ZSTK474 was approximately 20-fold stronger than that of LY294002. Another important feature of ZSTK474 is its high specificity for PI3K. When tested at 30 μ M, ZSTK474 did not inhibit the activity of 139 other

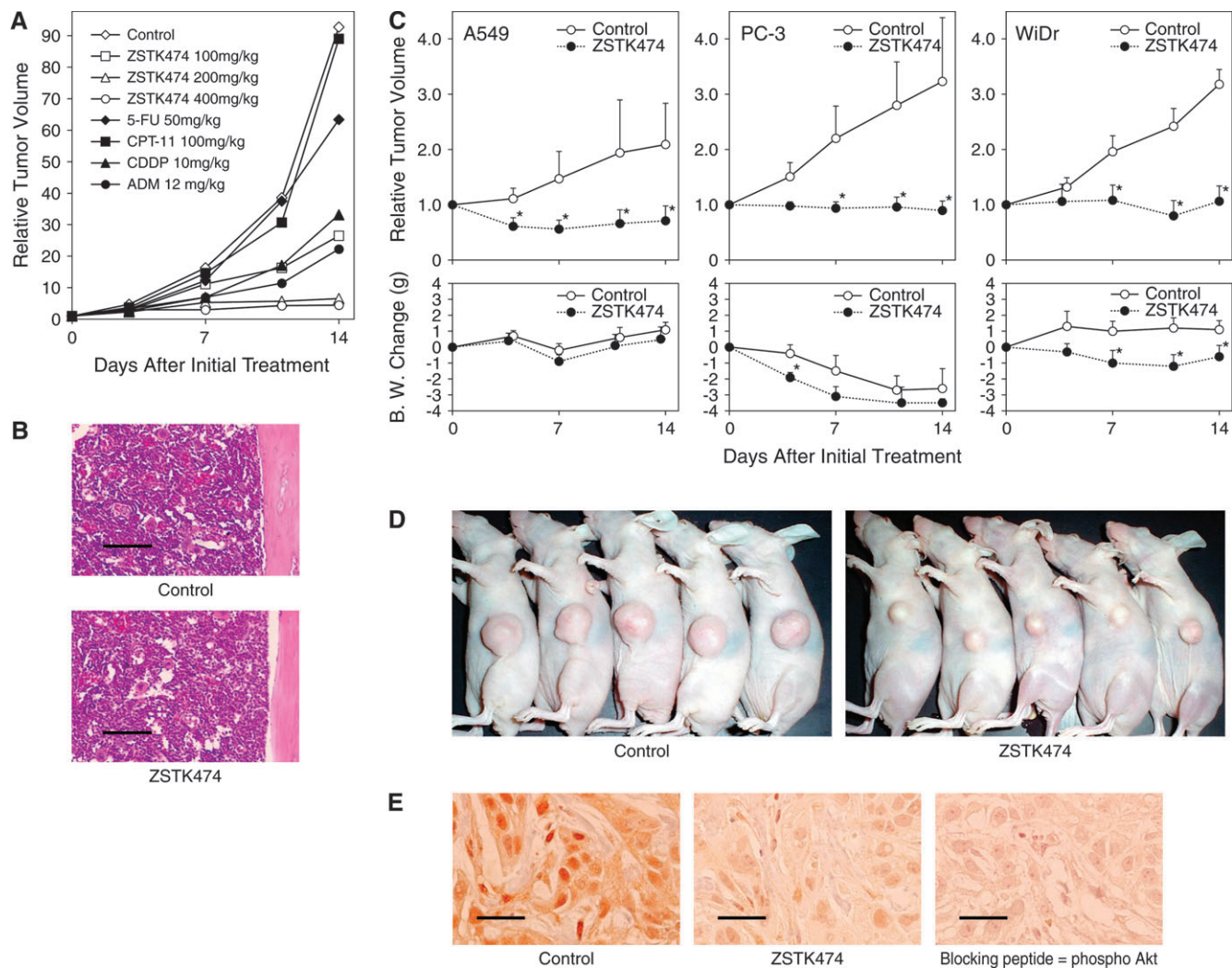


Fig. 8. Antitumor activity of ZSTK474. **A)** Antitumor activity of ZSTK474 against mouse B16F10 melanomas. Fifty-six BDF₁ mice were each subcutaneously injected with 5×10^5 B16F10 melanoma tumor cells. Seven days after inoculation, the administration of the drugs, as indicated, began (day 0). ZSTK474 was orally administered daily from days 0 to 13. Reference drugs were irinotecan (CPT-11), cisplatin (CDDP), doxorubicin (ADM), and 5-fluorouracil (5-FU). Each reference drug was administered intravenously from day 0 at the maximum tolerable dose by use of the following optimal schedules: CPT-11 at 100 mg/kg administered three times on days 0, 3, and 7; CDDP at 10 mg/kg once on day 0; ADM at 12 mg/kg once on day 0; and 5-FU at 50 mg/kg three times on days 0, 3, and 7. Each data point is the average of data from seven mice. **B)** Hematoxylin–eosin staining of femur bone marrow sections from BDF₁ mice bearing B16F10 melanomas 14 days after inoculation of tumor cells. ZSTK474 at 400 mg/kg was orally administered daily from days 0 to 13. **Scale bar** = 100 μ m. **C)** ZSTK474 and tumor growth and body weight in nude mice bearing human cancer xenografts. Forty-five nude mice were subcutaneously inoculated with a tumor fragment of 3 mm \times 3 mm \times 3 mm

from the subcutaneous tumor developed in nude mice. When tumors reached a volume of 100–300 mm³, animals were divided randomly into test groups, each with five mice (day 0). ZSTK474 (400 mg/kg) was orally administered daily from day 0 to 13 except for days 3 and 10. Data are the means of data from five mice. **Error bar** = the upper 95% confidence interval. **P* = .009, two-sided Mann–Whitney *U* test, compared with respective control. **D)** WiDr xenograft growth inhibition after administration of ZSTK474. ZSTK474 at 400 mg/kg was orally administered daily from days 0 to 26, except for days 6, 13, and 20. The mice were photographed on day 28. Other experimental conditions were the same as described above. **E)** ZSTK474 and Akt phosphorylation in nude mice bearing A549 human non–small-cell lung cancer xenografts. When the volume of tumors reached 100–300 mm³, ZSTK474 at 400 mg/kg was orally administered once. Mice were killed 4 hours after ZSTK474 administration, and excised tumors were analyzed by immunohistochemistry for the expression of phosphorylated Akt (Ser-473). Phosphorylated Akt (Ser-473) blocking peptide was incubated with phosphorylated Akt (Ser-473) antibody at 4 °C for 2 hours before incubating with the tissue section. **Scale bar** = 25 μ m.

protein kinases examined. The three-dimensional space in the ATP-binding pocket of PI3K is larger than the corresponding spaces found in the ATP-binding pockets of other protein kinases (44). The triazine and morpholino groups of ZSTK474 fit well into this space. Therefore, these moieties may be important in the specificity of ZSTK474 for PI3K. To further confirm the binding of ZSTK474 to the ATP-binding pocket of PI3K, a biochemical experiment that examines whether ZSTK474 competitively inhibits the binding of ATP to its binding site is required.

PI3K plays an important role in the proliferation of tumor cells. We compared ZSTK474 with other PI3K inhibitors, LY294002

and wortmannin, for its ability to inhibit cell proliferation. At concentrations of less than 1 μ M, ZSTK474 potently inhibited the growth of various cancer cell lines. The growth inhibitory activity of ZSTK474 was more than 10-fold stronger than that of wortmannin, which may be due to wortmannin's being somewhat unstable in cell culture medium (48), or of LY294002, which may be due to the PI3K inhibitory activity of LY294002 being more than 10-fold weaker than that of ZSTK474. Furthermore, the PI3K inhibitory activities of other *s*-triazine derivatives statistically significantly correlated with their cell growth inhibitory activities. These results suggested that ZSTK474 inhibited cell

growth by inhibiting PI3K, with subsequent inhibitory effects on downstream signaling molecules.

PI3K participates in the induction of the membrane ruffling. ZSTK474 inhibited platelet-derived growth factor–induced membrane ruffling in murine embryonic fibroblast cells, which is an Akt-independent process, and inhibited the generation of PIP₃. These results demonstrate that ZSTK474 inhibited PI3K activity in intact cells.

Because the PI3K pathway is considered to mediate antiapoptotic signals in tumor cells, ZSTK474 was expected to induce apoptosis efficiently by inhibiting PI3K. However, we observed weak or no induction of apoptosis after ZSTK474 treatment in OVCAR3 cells or A549 cells, respectively. Therefore, induction of apoptosis by ZSTK474 appears to be a cell type–dependent event, probably because of the differential status of the PI3K signaling pathway in various cancer cell lines.

One of the major downstream effectors of PI3K is Akt, a serine/threonine protein kinase. Therefore, we investigated the effect of PI3K on the activation of Akt and its key downstream components. ZSTK474 reduced, in a time-dependent manner, phosphorylation of the protein kinases Akt and GSK-3 β and the expression of cyclin D1 protein. Akt inhibits cyclin D1 degradation by regulating the activity of GSK-3 β (49). After its phosphorylation by GSK-3 β , cyclin D1 is targeted for degradation by the proteasome. Akt phosphorylates GSK-3 β directly and blocks its kinase activity, thereby allowing cyclin D1 to accumulate in cells (49). ZSTK474 inhibited the phosphorylation of other downstream signaling components that are involved in regulating cell proliferation (i.e., FKHRL1, FKHR, TSC-2, mTOR, and p70S6K) in a dose-dependent manner. These results indicated that the inhibition of PI3K by ZSTK474 was followed by a decrease in relevant downstream signaling, which may in turn facilitate cell growth inhibition. In fact, we observed complete G₁-phase arrest in A549 cells after ZSTK474 treatment. In contrast, ZSTK474 did not inhibit phosphorylation of either ERK1/2 or MEK1/2, suggesting that ZSTK474 does not inhibit components in the RAS–ERK pathway.

Orally administered ZSTK474 displayed potent antitumor activity against human cancer xenografts in mice, without evidence of critical toxicity. Known PI3K inhibitors—such as LY294002 (46,50–52), wortmannin (53,54), and viridin analogues (54)—have previously been examined for their antitumor activities. In most reports, LY294002, which was administered intraperitoneally because it is insoluble in water, had antitumor activity when administered at an early stage (i.e., within 7 days after inoculation of tumor cells) (50), but it also induced severe dermal toxicity (46). Wortmannin also had antitumor activity, but again it achieved sufficient efficacy only when administered at an early stage (53), and it caused liver toxicity (54). An analogue of wortmannin, PX-866, has recently been developed (54) that has better efficacy and lower toxicity than wortmannin. However, this agent still produces liver toxicity (54). In this study, we found that ZSTK474 had strong antitumor efficacy against advanced-stage tumors (i.e., >15 days after inoculation of tumor cells) and that ZSTK474 did not produce noticeable toxicity in critical organs after daily administration for more than 14 days. We also confirmed reduction of Akt phosphorylation after ZSTK474 administration. Thus, the reduction of Akt phosphorylation may be a useful biomarker marker to monitor the efficacy of ZSTK474 in future investigations of ZSTK474.

Although ZSTK474 indicated favorable features for a novel anticancer drug candidate as described above, various preclinical

studies remain before ZSTK474 can be evaluated in a clinical trial, which include more precise investigation of the molecular pharmacology, analyses of the pharmacokinetics and the pharmacodynamics, and careful investigation of the toxicity. Investigation of the toxicity derived from PI3K inhibition is especially important because PI3K is expressed in various normal tissues. These studies are currently under way.

In conclusion, we demonstrated that the compound ZSTK474 is a new PI3K inhibitor and that it has strong antitumor activity against human cancer xenografts without critical toxicity. It appears that ZSTK474 can be orally administered over long periods, which may be important for the treatment of cancer. Thus, ZSTK474 merits further investigation as an anticancer drug.

REFERENCES

- (1) Auger KR, Serunian LA, Soltoff SP, Libby P, Cantley LC. PDGF-dependent tyrosine phosphorylation stimulates production of novel polyphosphoinositides in intact cells. *Cell* 1989;57:167–75.
- (2) Whitman M, Downes CP, Keeler M, Keller T, Cantley L. Type I phosphatidylinositol kinase makes a novel inositol phospholipid, phosphatidylinositol-3-phosphate. *Nature* 1988;332:644–6.
- (3) Vivanco I, Sawyers CL. The phosphatidylinositol 3-Kinase AKT pathway in human cancer. *Nat Rev Cancer* 2002;2:489–501.
- (4) Luo J, Manning BD, Cantley LC. Targeting the PI3K-Akt pathway in human cancer: rationale and promise. *Cancer Cell* 2003;4:257–62.
- (5) Aoki M, Schetter C, Himly M, Batista O, Chang HW, Vogt PK. The catalytic subunit of phosphoinositide 3-kinase: requirements for oncogenicity. *J Biol Chem* 2000;275:6267–75.
- (6) Jimenez C, Jones DR, Rodriguez-Viciana P, Gonzalez-Garcia A, Leonardo E, Wennstrom S, et al. Identification and characterization of a new oncogene derived from the regulatory subunit of phosphoinositide 3-kinase. *EMBO J* 1998;17:743–53.
- (7) Samuels Y, Wang Z, Bardelli A, Silliman N, Ptak J, Szabo S, et al. High frequency of mutations of the PIK3CA gene in human cancers. *Science* 2004;304:554.
- (8) Levine DA, Bogomolny F, Yee CJ, Lash A, Barakat RR, Borgen PI, et al. Frequent mutation of the PIK3CA gene in ovarian and breast cancers. *Clin Cancer Res* 2005;11:2875–8.
- (9) Shayesteh L, Lu Y, Kuo WL, Baldocchi R, Godfrey T, Collins C, et al. PIK3CA is implicated as an oncogene in ovarian cancer. *Nat Genet* 1999;21:99–102.
- (10) Pedrero JM, Carracedo DG, Pinto CM, Zapatero AH, Rodrigo JP, Nieto CS, et al. Frequent genetic and biochemical alterations of the PI 3-K/AKT/PTEN pathway in head and neck squamous cell carcinoma. *Int J Cancer* 2005;114:242–8.
- (11) Kobayashi M, Nagata S, Iwasaki T, Yanagihara K, Saitoh I, Karouji Y, et al. Dedifferentiation of adenocarcinomas by activation of phosphatidylinositol 3-kinase. *Proc Natl Acad Sci U S A* 1999;96:4874–9.
- (12) Steck PA, Pershouse MA, Jasser SA, Yung WK, Lin H, Ligon AH, et al. Identification of a candidate tumour suppressor gene, MMAC1, at chromosome 10q23.3 that is mutated in multiple advanced cancers. *Nat Genet* 1997;15:356–62.
- (13) Lee HY, Srinivas H, Xia D, Lu Y, Superty R, LaPushin R, et al. Evidence that phosphatidylinositol 3-kinase- and mitogen-activated protein kinase kinase-4/c-Jun NH2-terminal kinase-dependent pathways cooperate to maintain lung cancer cell survival. *J Biol Chem* 2003;278:23630–8.
- (14) Czauderna F, Fechtner M, Aygun H, Arnold W, Klippel A, Giese K, et al. Functional studies of the PI(3)-kinase signalling pathway employing synthetic and expressed siRNA. *Nucleic Acids Res* 2003;31:670–82.
- (15) Okada T, Sakuma L, Fukui Y, Hazeki O, Ui M. Blockage of chemotactic peptide-induced stimulation of neutrophils by wortmannin as a result of selective inhibition of phosphatidylinositol 3-kinase. *J Biol Chem* 1994;269:3563–7.
- (16) Powis G, Bonjouklian R, Berggren MM, Gallegos A, Abraham R, Ashendel C, et al. Wortmannin, a potent and selective inhibitor of phosphatidylinositol-3-kinase. *Cancer Res* 1994;54:2419–23.

- (17) Wipf P, Minion DJ, Halter RJ, Berggren MI, Ho CB, Chiang GG, et al. Synthesis and biological evaluation of synthetic viridins derived from C(20)-heteroalkylation of the steroidal PI-3-kinase inhibitor wortmannin. *Org Biomol Chem* 2004;2:1911–20.
- (18) Woscholski R, Kodaki T, McKinnon M, Waterfield MD, Parker PJ. A comparison of demethoxyviridin and wortmannin as inhibitors of phosphatidylinositol 3-kinase. *FEBS Lett* 1994;342:109–14.
- (19) Vlahos CJ, Matter WF, Hui KY, Brown RF. A specific inhibitor of phosphatidylinositol 3-kinase, 2-(4-morpholinyl)-8-phenyl-4H-1-benzopyran-4-one (LY294002). *J Biol Chem* 1994;269:5241–8.
- (20) West KA, Castillo SS, Dennis PA. Activation of the PI3K/Akt pathway and chemotherapeutic resistance. *Drug Resist Updat* 2002;5:234–48.
- (21) Workman P. Inhibiting the phosphoinositide 3-kinase pathway for cancer treatment. *Biochem Soc Trans* 2004;32:393–6.
- (22) Yaguchi S, Izumisawa Y, Sato M, Nakagane T, Koshimizu I, Sakita K, et al. In vitro cytotoxicity of imidazolyl-1,3,5-triazine derivatives. *Biol Pharm Bull* 1997;20:698–700.
- (23) Matsuno T, Karo M, Sasahara H, Watanabe T, Inaba M, Takahashi M, et al. Synthesis and antitumor activity of benzimidazolyl-1,3,5-triazine and benzimidazolylpyrimidine derivatives. *Chem Pharm Bull (Tokyo)* 2000;48:1778–81.
- (24) Dan S, Tsunoda T, Kitahara O, Yanagawa R, Zembutsu H, Katagiri T, et al. An integrated database of chemosensitivity to 55 anticancer drugs and gene expression profiles of 39 human cancer cell lines. *Cancer Res* 2002;62:1139–47.
- (25) Yamori T. Panel of human cancer cell lines provides valuable database for drug discovery and bioinformatics. *Cancer Chemother Pharmacol* 2003; 52 Suppl 1:S74–9.
- (26) Yamori T, Matsunaga A, Sato S, Yamazaki K, Komi A, Ishizu K, et al. Potent antitumor activity of MS-247, a novel DNA minor groove binder, evaluated by an in vitro and in vivo human cancer cell line panel. *Cancer Res* 1999;59:4042–9.
- (27) Monks A, Scudiero D, Skehan P, Shoemaker R, Paull K, Vistica D, et al. Feasibility of a high-flux anticancer drug screen using a diverse panel of cultured human tumor cell lines. *J Natl Cancer Inst* 1991;83:757–66.
- (28) Paull KD, Shoemaker RH, Hodes L, Monks A, Scudiero DA, Rubinstein L, et al. Display and analysis of patterns of differential activity of drugs against human tumor cell lines: development of mean graph and COMPARE algorithm. *J Natl Cancer Inst* 1989;81:1088–92.
- (29) Fidler IJ. Biological behavior of malignant melanoma cells correlated to their survival in vivo. *Cancer Res* 1975;35:218–24.
- (30) Skehan P, Storeng R, Scudiero D, Monks A, McMahon J, Vistica D, et al. New colorimetric cytotoxicity assay for anticancer-drug screening. *J Natl Cancer Inst* 1990;82:1107–12.
- (31) Boyd MR. Status of the National Cancer Institute preclinical antitumor drug discovery screen: implications for selection of new agents for clinical trial. Vol 3. Philadelphia (PA): Lippincott; 1989.
- (32) Fukui Y, Kornbluth S, Jong SM, Wang LH, Hanafusa H. Phosphatidylinositol kinase type I activity associates with various oncogene products. *Oncogene Res* 1989;4:283–92.
- (33) Gray A, Olsson H, Batty IH, Priganica L, Peter Downes C. Nonradioactive methods for the assay of phosphoinositide 3-kinases and phosphoinositide phosphatases and selective detection of signaling lipids in cell and tissue extracts. *Anal Biochem* 2003;313:234–45.
- (34) Rarey M, Kramer B, Lengauer T, Klebe G. A fast flexible docking method using an incremental construction algorithm. *J Mol Biol* 1996;261:470–89.
- (35) Tsujishita H, Hirono S. CAMDAS: an automated conformational analysis system using molecular dynamics. *Conformational Analyzer with Molecular Dynamics And Sampling. J Comput Aided Mol Des* 1997;11:305–15.
- (36) Radwan AA, Gouda H, Yamaotsu N, Torigoe H, Hirono S. Rational procedure for 3D-QSAR analysis using TRNOE experiments and computational methods: application to thermolysin inhibitors. *Drug Des Discov* 2001;17:265–81.
- (37) Kuntz ID, Blaney JM, Oatley SJ, Langridge R, Ferrin TE. A geometric approach to macromolecule-ligand interactions. *J Mol Biol* 1982;161:269–88.
- (38) Jones G, Willett P, Glen RC, Leach AR, Taylor R. Development and validation of a genetic algorithm for flexible docking. *J Mol Biol* 1997;267:727–48.
- (39) Eldridge MD, Murray CW, Auton TR, Paolini GV, Mee RP. Empirical scoring functions: I. The development of a fast empirical scoring function to estimate the binding affinity of ligands in receptor complexes. *J Comput Aided Mol Des* 1997;11:425–45.
- (40) Muegge I, Martin YC. A general and fast scoring function for protein-ligand interactions: a simplified potential approach. *J Med Chem* 1999;42:791–804.
- (41) Katsuki M, Chuang VT, Nishi K, Kawahara K, Nakayama H, Yamaotsu N, et al. Use of photoaffinity labeling and site-directed mutagenesis for identification of the key residue responsible for extraordinarily high affinity binding of UCN-01 in human alpha1-acid glycoprotein. *J Biol Chem* 2005;280:1384–91.
- (42) Kimura K, Hattori S, Kabuyama Y, Shizawa Y, Takayanagi J, Nakamura S, et al. Neurite outgrowth of PC12 cells is suppressed by wortmannin, a specific inhibitor of phosphatidylinositol 3-kinase. *J Biol Chem* 1994;269:18961–7.
- (43) Plank J, Rychlo A. [A method for quick decalcification.]. *Zentralbl Allg Pathol* 1952;89:252–4.
- (44) Walker EH, Pacold ME, Perisic O, Stephens L, Hawkins PT, Wymann MP, et al. Structural determinants of phosphoinositide 3-kinase inhibition by wortmannin, LY294002, quercetin, myricetin, and staurosporine. *Mol Cell* 2000;6:909–19.
- (45) Lawrie AM, Noble ME, Tunnah P, Brown NR, Johnson LN, Endicott JA. Protein kinase inhibition by staurosporine revealed in details of the molecular interaction with CDK2. *Nat Struct Biol* 1997;4:796–801.
- (46) Hu L, Zaloudek C, Mills GB, Gray J, Jaffe RB. In vivo and in vitro ovarian carcinoma growth inhibition by a phosphatidylinositol 3-kinase inhibitor (LY294002). *Clin Cancer Res* 2000;6:880–6.
- (47) Naasani I, Seimiya H, Yamori T, Tsuruo T. FJ5002: a potent telomerase inhibitor identified by exploiting the disease-oriented screening program with COMPARE analysis. *Cancer Res* 1999;59:4004–11.
- (48) Holleran JL, Egorin MJ, Zuhowski EG, Parise RA, Musser SM, Pan SS. Use of high-performance liquid chromatography to characterize the rapid decomposition of wortmannin in tissue culture media. *Anal Biochem* 2003;323:19–25.
- (49) Diehl JA, Cheng M, Roussel MF, Sherr CJ. Glycogen synthase kinase-3beta regulates cyclin D1 proteolysis and subcellular localization. *Genes Dev* 1998;12:3499–511.
- (50) Su JD, Mayo LD, Donner DB, Durden DL. PTEN and phosphatidylinositol 3'-kinase inhibitors up-regulate p53 and block tumor-induced angiogenesis: evidence for an effect on the tumor and endothelial compartment. *Cancer Res* 2003;63:3585–92.
- (51) Semba S, Itoh N, Ito M, Harada M, Yamakawa M. The in vitro and in vivo effects of 2-(4-morpholinyl)-8-phenyl-chromone (LY294002), a specific inhibitor of phosphatidylinositol 3'-kinase, in human colon cancer cells. *Clin Cancer Res* 2002;8:1957–63.
- (52) Bondar VM, Sweeney-Gotsch B, Andreeff M, Mills GB, McConkey DJ. Inhibition of the phosphatidylinositol 3'-kinase-AKT pathway induces apoptosis in pancreatic carcinoma cells in vitro and in vivo. *Mol Cancer Ther* 2002;1:989–97.
- (53) Lemke LE, Paine-Murrieta GD, Taylor CW, Powis G. Wortmannin inhibits the growth of mammary tumors despite the existence of a novel wortmannin-insensitive phosphatidylinositol-3-kinase. *Cancer Chemother Pharmacol* 1999;44:491–7.
- (54) Ihle NT, Williams R, Chow S, Chew W, Berggren MI, Paine-Murrieta G, et al. Molecular pharmacology and antitumor activity of PX-866, a novel inhibitor of phosphoinositide-3-kinase signaling. *Mol Cancer Ther* 2004;3:763–72.

NOTES

We thank Dr. R. H. Shoemaker and Dr. K. D. Paull for discussion on the establishment of JFCR39 and COMPARE analysis; Ms. Y. Nishimura, Ms. M. Seki, Ms. Y. Mukai, Ms. M. Okamura, and Dr. Y. Yoshida for technical assistance; Mr. T. Watanabe, Dr. Y. Tsuchida and Mr. K. Saito for synthesis of compounds; and Mr. M. Takehara and Dr. M. Takahashi for advice on the study.

Supported by grants-in-aid of the Priority Area “Cancer” from the Ministry of Education, Culture, Sports, Science, and Technology, Japan, to T. Yamori (11177101); grants-in-aid for Scientific Research (B) from Japan Society for the Promotion of Science to T. Yamori (17390032); and a grant from National Institute of Biomedical Innovation, Japan, to T. Yamori (05-13).

Funding to pay the Open Access publication charges for this article was provided by the Japanese Foundation for Cancer Research.

Manuscript received September 16, 2005; revised January 23, 2006; accepted March 3, 2006.